A Geometrical Explanation for the Enhanced Small-Scale Roughness of a Liquid Surface

Leon F. Phillips†

Chemistry Department, Rowland Hall, University of California, Irvine, California 92612

Received: September 18, 2003; In Final Form: December 1, 2003

The small-scale motion of a liquid surface is discussed in terms of the behavior of Gaussian local modes when the discrete molecular structure of the surface becomes important. The observed enhancement of surface roughness as the scale of observation approaches molecular dimensions is attributed to the transition from purely harmonic motion, with restoring force parallel to the surface, to anharmonic motion, with restoring force at right angles to the surface. Calculations based on this model, with no adjustable parameters, give results in excellent agreement with experimental data for the initial decrease and subsequent increase of the apparent surface tension with increasing wave vector, and for the variation of surface tension versus wave vector plots with the nature of the liquid. Because the important intermolecular interactions in the model occur at short range, there is very little difference between the results predicted for $1/r^3$ and $1/r^6$ potentials. The increase in apparent surface tension as the wave vector approaches its upper limit is the consequence of thermally excited motion on this scale frequently exceeding the potential barriers that otherwise would prevent either evaporation of the molecules involved or their accommodation into the bulk liquid, with the result that such large-amplitude motions do not contribute to the time-averaged surface roughness.

Introduction

On a molecular scale, the surface of a liquid is a zone of rapid, chaotic motion, where condensing and evaporating molecules continually arrive and depart and the measured values of bulk quantities such as density vary continuously, over a distance of the order of a few tens of angstroms, from the value characteristic of the liquid to the value characteristic of the gas. This is, however, a time-averaged view. Without time averaging, the currently accepted picture of the gas−liquid interface is that the boundary between gas and liquid is well-defined at any instant, but its location is highly variable in both time and space as the result of the superposition of a large number of thermally excited capillary waves.[1]

Capillary waves are waves in the uniform elastic membrane produced by surface tension, so the description in terms of capillary waves must break down on distance scales at which the discrete molecular structure of the surface is important. If the behavior of individual molecules is the main interest, the surface can be treated by molecular dynamics calculations,[2] but such calculations are presently limited to slabs containing a few hundred molecules, so the regions of applicability of the discrete and continuum models do not overlap. This paper attempts to bridge the gap between the domains of molecular dynamics calculations and capillary-wave theory by considering the collective motion of groups of up to several hundred molecules in the top few surface layers of a liquid. In the process of bridging the gap, it generates a new and remarkably simple treatment of the factors responsible for the observed enhancement in surface roughness as the scale of the observations approaches molecular dimensions.[3]

The capillary-wave spectrum is often expressed in terms of products of circular functions of the form

$$\zeta_\omega = A_\omega \cos(\omega t + kx + \delta_x) \cos(\omega t + ky + \delta_y) \qquad (1)$$

where ζ_ω is the displacement of the surface from its mean position due to the mode of circular frequency ω, the x and y coordinate axes are parallel to the mean surface, the quantities δ_i are phase shifts, and $k = 2\pi/\lambda$ is the wave vector. However, other sets of basis functions can be both more convenient and more realistic. Examples include the use of spherical harmonics to describe the normal vibrations of a droplet surface,[4] and of Bessel functions $J_0(kr)$ to describe the over-damped local modes that dominate the high-frequency spectrum of a flat surface.[5] At large r the Bessel function has the limiting form $(2/kr)^{1/2} \cos(kr - \pi/4)$, which allows the parameter k to continue to be termed the wave vector and provides a mechanism for local impacts to excite normal modes. The choice of basis set makes no difference to derived quantities such as height−height correlations or the root-mean-square (rms) displacement of the surface from its mean position, which is about 3.8×10^{-8} cm for a water surface at 300 K. The location of the surface is normally distributed, so this value of the rms displacement indicates that the surface location lies within a zone 15.2 Å wide for 95% of the time.

Mecke and co-workers[3,6,7] have investigated the time-averaged small-scale roughness of liquid surfaces both experimentally, by synchrotron X-ray scattering, and theoretically, using density functional theory. Their experimental results for a variety of liquids—Octamethylcyclotetrasiloxane (OMCTS), carbon tetrachloride, squalane, ethylene glycol, and water—are strikingly similar. All show a marked increase in surface roughness over the value predicted by capillary-wave theory at k-values greater than about 3×10^6 cm^{-1}, the roughness decreasing again when k is close to the upper limit that is set by the molecular diameter. In parallel to the change in surface roughness, the apparent surface tension value falls to about half the macroscopic value at large k, then rises sharply at very large k. These observations amount to a clear and unambiguous demonstration of the

† Permanent address: Chemistry Department, University of Canterbury, Christchurch, New Zealand.

10.1021/jp036781i CCC: $27.50
Published on Web 01/20/2004

departure of the surface motion from the predictions of capillary-wave theory on short distance scales, and the observed k-dependence of surface tension provides an invaluable testing ground for theory.

In their theoretical treatment,[7] Mora et al. were able to model the variation of surface roughness with k for all of the liquids studied with the assumption of a Lennard-Jones intermolecular potential in every case. This result is quite surprising, because the long-range part of the potential was considered to be particularly important in their treatment and the Lennard-Jones potential varies as $1/r^6$ at long range, whereas the properties of hydrogen-bonded liquids such as water and glycol are dominated by the dipole−dipole potential, which varies as $1/r^3$ at long range.[8−10] The effective value of the dipole moment of liquid water is significantly enhanced over the gas-phase value,[11] so their suggestion that "orientational-smearing by thermal averaging" renders the dipole−dipole interaction inoperative is not convincing.

The present paper provides an alternative explanation for the increased surface roughness at high k values, in terms of a change in the nature of the restoring force between high-k and low-k deformations of the surface. The change occurs for purely geometrical reasons as the horizontal extent of a surface deformation decreases to the point where it is comparable with both the vertical amplitude of the motion and the effective diameter of the molecular units that make up the surface. With the present model, the small-scale motion of the surface is controlled by the interactions between adjacent molecules in a quasi-close-packed liquid. As a result, the predictions of the model are almost independent of the nature of the long-range potential, which is in accord with the experimental data of Mora et al.[7] The model also suggests some new insights into the processes of evaporation and accommodation.

Surface Displacement Model

The surface motions of interest occur at k-values which are well above the critical damping value $k_c = \rho\gamma/\eta^2$ for normal modes (7.3×10^5 cm^{-1} on water at 300 K), so the most suitable capillary-wave basis functions are radially symmetric local modes[5] of the form

$$\zeta_k = A_k\{1 - \exp(-t/\tau_{rise})\} \exp(-t/\tau_{fall})\}J_0(kr) \qquad (2)$$

where $J_0(kr)$ is a Bessel function of the radius r in units $1/k$, the rise-time τ_{rise} is equal to $\pi/2k^2\eta$, and the fall-time τ_{fall} is $2\eta/k\gamma$, where ρ = density, γ = surface tension, and η = viscosity, and the amplitude factor A_k can be positive or negative. Both of the characteristic times decrease with increasing k, the rise-time decreasing more rapidly than the fall-time. The ratio τ_{rise}/τ_{fall} is equal to (5.7×10^5cm$^{-1}/k$) for water at 300 K, which means that the rise-time is always shorter than the fall-time for local modes on water at 300 K, and is *much* shorter than the fall-time at values of k near the maximum value of $\sim 1.6 \times 10^8$ cm^{-1}. It follows that, on a small distance scale, the surface spends most of its time in the falling phases of a large number of overlapping local modes which are excited by sudden positive- or negative-going impacts due to the thermal motion of molecules below the surface.

Any arbitrary displacement of the surface with radial symmetry can be expressed as a Fourier−Bessel series in terms of the basis set $J_0(kr)$. The Fourier−Bessel components of a Gaussian dome (the solid obtained by rotating a Gaussian function $y = \exp(-x^2/2\langle x^2\rangle)$ about the y axis) are clustered together near the lower end of the available range of k values[5] so that, because the high-k components of an arbitrary deformation decay more rapidly than low-k components, the slowly falling phase of any arbitrary displacement tends to resemble a Gaussian dome. We choose a Gaussian dome as the model for a surface displacement at high k values for this reason and because a Gaussian falls to zero much more rapidly than a Bessel J_0 function.

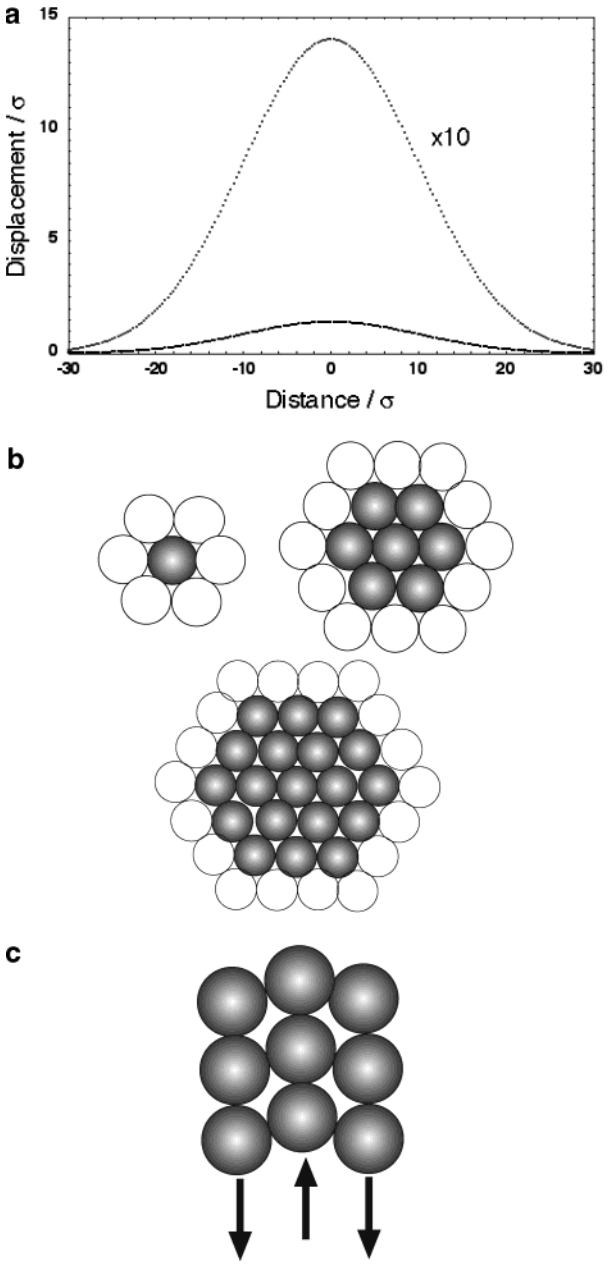

Figure 1. (a) Diagram of a section through a Gaussian mode whose radius is much greater than the molecular diameter σ. Note the different horizontal and vertical scales. (b) Plan view of small close-packed domes. (c) Cross-section of three layers for the smallest dome of panel b.

For an isolated Gaussian dome whose radius is greater than its height and whose total energy is k_BT, the root-mean-square vertical displacement is 1.34×10^{-8} cm.[5] For a dome such as the one shown in cross-section in Figure 1a, where the radius is so much larger than the molecular diameter that the presence of discrete molecules is not evident and the peak vertical displacement is much smaller than the radius of the disturbance, the restoring force that we attribute to surface tension is

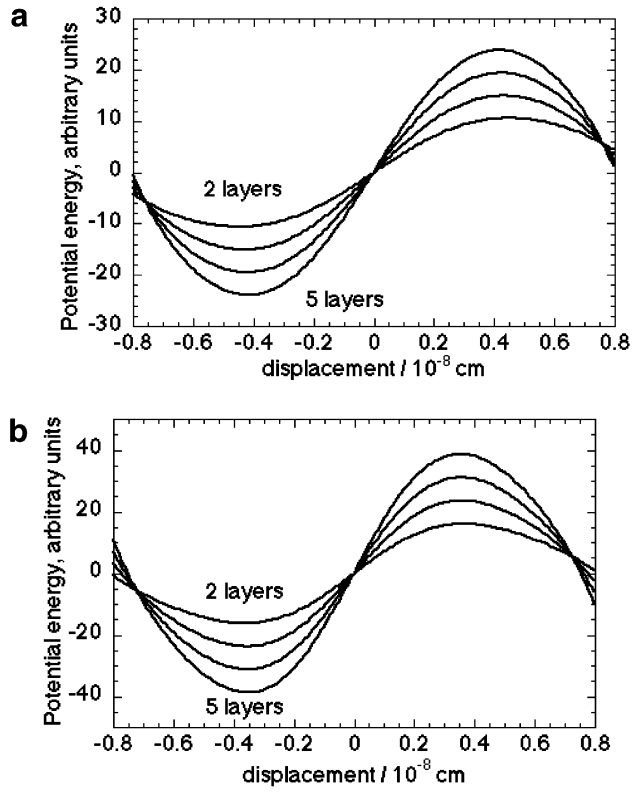

Figure 2. (a) Variation of potential energy (in arbitrary units) with displacement for the dome of Figure 1b, with a $1/r^3$ potential, for different numbers of layers of molecules included in the vertical motion. (b) As for panel a, but with a $1/r^6$ potential.

tangential to the local surface and remains almost parallel to the mean surface during the dome's rise and fall. The relative displacement of two adjacent surface molecules is extremely small when the surface is stretched in this way, so this type of motion is inherently harmonic and well-described by capillary-wave theory. That is in marked contrast to the limiting case of a small Gaussian dome, of which some examples are shown in plan view in Figure 1b for a quasi-close-packed surface. The most extreme case is shown in cross-section in Figure 1c, for motion involving three layers of molecules at the surface. Here the restoring force is perpendicular to the surface, the nominal rms displacement given by capillary-wave theory is comparable with the molecular radius, and the motion is inherently anharmonic.

One might expect the restoring force for the vertical displacement in Figure 1c to depend on both the nature of the intermolecular potential and the number of layers of quasi-close-packed molecules that are involved in the moving vertical column. However, the results of calculations for concerted motions of 2, 3, 4, and 5 layers, shown in Figure 2a for an arbitrary $1/r^3$ potential and in Figure 2b for an arbitrary $1/r^6$ potential, show that the qualitative form of the potential is not altered significantly by varying either the type of long-range potential or the number of layers involved in the motion. Also, varying the distance between a central molecule in one layer and the stationary molecules in the layer below, as would be required if the six-membered rings were rotated relative to one another to achieve closer packing, makes no significant difference. The variation of potential energy with displacement is far from quadratic, being approximately linear for displacements smaller than about 1×10^{-9} cm, i.e., much less than the rms value. For larger displacements the effective force constant decreases rapidly, and for displacements greater than about 8×10^{-9} cm the potential changes sign, behavior that has some interesting implications in relation to evaporation and accommodation.

Calculations

The motion in Figure 1c represents the extreme case of small-scale motion at right angles to the surface, but similar considerations should apply to the other small domes in Figure 1b. It is therefore of interest to calculate the contribution of displacements with restoring force perpendicular to the surface to the motion of Gaussian domes of intermediate and larger size.

For these calculations the effective dome radius was chosen to be twice the rms radius of the parent Gaussian, on the grounds that the farther reaches of the dome would inevitably be confused by the presence of other local modes. The dome radius was fixed at $(n_r - 0.5)$ times the molecular diameter σ, where the positive integer n_r was one unit larger than the number of cylindrical zones, each one molecule thick, surrounding the central core of molecules in a dome of the kind shown in Figure 1b. The minimum k-value was then given by $2.4048/\{(n_r - 0.5)\sigma\}$, where the factor 2.4048 and the value 0.5 derive from the fact that the dome with the highest possible k-value is essentially a pure Bessel $J_0(kr)$ function, whose first zero, at $kr = 2.4048$, must occur at $r = \sigma/2$. In principle, the effective k-value of a Gaussian dome could be calculated as the average k-value for all of the Fourier−Bessel components of the dome. This approach was tried and discarded because the value so obtained is strongly dependent on the choice of radius for the circular zone over which the Fourier−Bessel expansion is to apply. Instead, and partly to give closer correspondence with the work of Mora et al.,[7] the k-value was obtained from the first term of a Fourier cosine expansion for the dome by taking the maximum radius to be $\lambda/2$. The nature of the final conclusions does not depend significantly on these choices.

The Gaussian profile was calculated for a range of heights up to about 10 times the rms displacement for an isolated Gaussian dome on the liquid at 300 K. At each height the relative displacements between adjacent pairs of molecules along the profile were calculated and used to calculate the increase in the total potential energy of the dome due to the displacement. This was done for a skin comprising a fixed number of layers of initially quasi-close-packed molecules, where the number of layers was normally chosen to be an integer in the range 2 to 5. As with the calculations that led to Figure 2, the nature of the final results did not depend significantly on the number of layers.

Consider the dome resulting from a positive displacement. First the potential energy was calculated for the central molecular column interacting with the surrounding cylinder (whose height was equal to one more than the chosen number of layers) for both $1/r^3$ and $1/r^6$ potentials, by the same procedure as was used to obtain the results in Figure 2. Then, for each successive cylinder of molecules outside the central column, the attraction to molecules in the same cylinder was assumed to remain constant during the motion, while the attraction to molecules inside the cylinder had already been calculated in the previous step. Every molecule in the cylinder was then assumed to be attracted to two adjacent molecules in the next outer ring and initially at the same level, to two molecules in the next outer ring and one level lower, if that level was being included in the calculation, and to two molecules in the next outer ring and one level higher, if the molecule under consid-

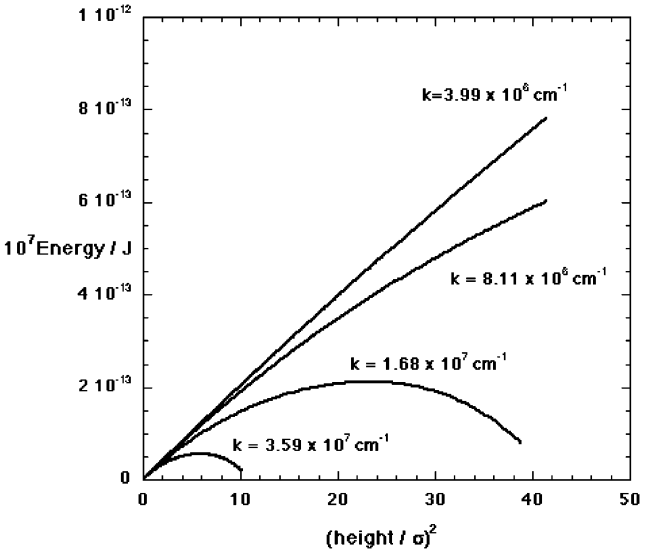

Figure 3. Energy plotted against the square of the peak displacement of a water surface for several values of the wave vector *k*. For a purely harmonic motion such plots are linear.

eration was below the surface layer. This is obviously a very simple model, with no consideration of the radial distribution function of the liquid. It would not have been difficult to include additional pairwise potentials, but that was thought to be unjustified in view of the other manifest limitations of the calculations. The potential energies so obtained all varied with the motion because of the relative vertical displacement of the successive rings. The number of molecules in each ring was calculated by dividing the circumference of the ring by the molecular diameter and truncating the result to an integer. A little consideration shows that exactly the same algorithm can be used for the depression resulting from a negative displacement.

For each value of dome height (or depth) the potential energy contributions were summed and the value obtained with zero vertical displacement was subtracted. When the radius parameter n_r was greater than about 30 the calculated energies were accurately proportional to the square of the peak displacement and the motion was harmonic. For smaller values of n_r this was not true, the effective force constant decreasing with increasing amplitude. For values of n_r less than about 10 the energy passed through a maximum and the calculation was stopped automatically just before the potential energy became negative. Energy values beyond the energy maximum were not included in the calculations. For a positive displacement, excitation over the maximum would cause one or more layers of the molecules involved to evaporate and therefore not be available to contribute to the surface roughness. Similarly, for a negative displacement, the molecules at the peak of the displacement would become incorporated in the next lower layer and the depth would remain at the limiting value for the energy maximum. Some representative plots of energy versus the square of the dome height for the water $1/r^3$ potential are given in Figure 3. The plots in Figure 3 correspond to $n_r = 32$, 16, 8 and 4.

TABLE 1: Liquid Parameters

molecule	surface tension, mN/m	molecular diameter, cm
OMCTS	18	7.9×10^{-8}
CCl_4	30	6.2×10^{-8}
squalane	28	10.1×10^{-8}
water	73	2.5×10^{-8}
ethylene glycol	46	4.4×10^{-8}

The next step in the calculation was to fit E/h^2, the energy divided by the square of the dome height, to a fifth-order polynomial in h^2. This enabled the potential energy for any displacement to be accurately scaled to the rms displacement of 1.34×10^{-8} cm, which in turn was scaled to half the thermal energy k_BT, where k_B is Boltzmann's constant and the quantity k_BT is evenly divided between potential and kinetic energy. The Boltzmann factors giving the relative probabilities of the different h^2 values, and hence the thermally averaged value of h^2, could then be calculated. This procedure involved the reasonable assumption that energy rather than free energy was the appropriate variable for this system. For cases where the potential energy decreased with increasing height, the probabilities of height values on the decreasing arm of the curve were set to zero since, as already noted, the attempt to achieve such heights would result in part of the dome either being lost by evaporation, in the case of a positive displacement, or becoming incorporated in the liquid below the surface layers, in the case of a negative displacement.

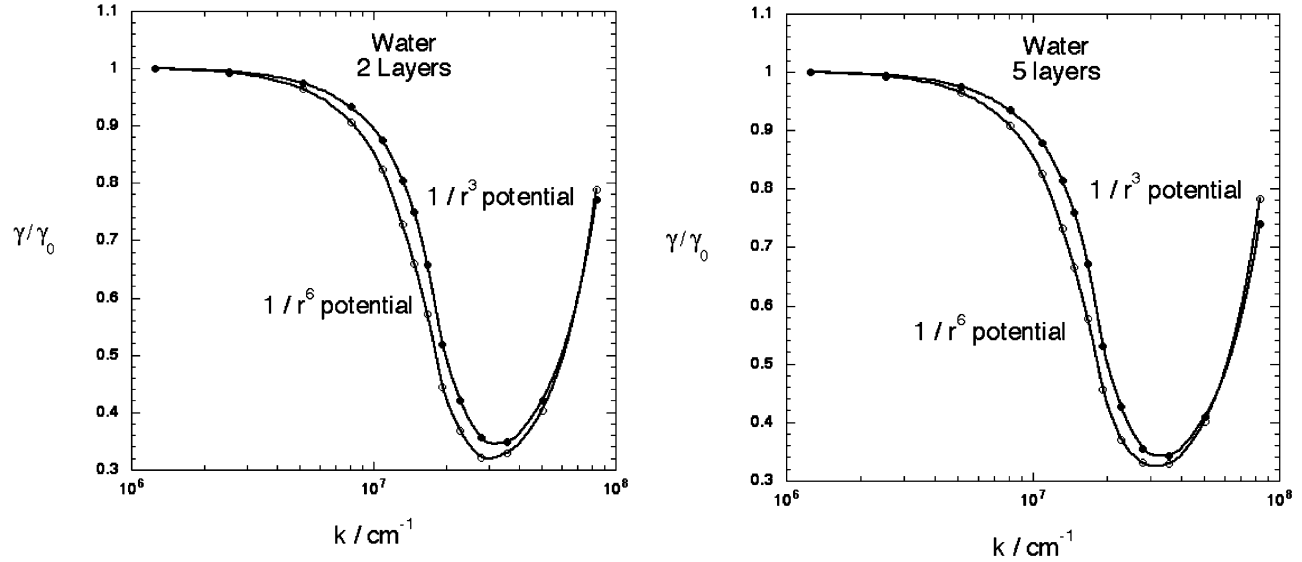

Figure 4. (a) Predicted dependence of the surface tension ratio γ/γ_0 on the wave vector, where γ_0 is the macroscopic surface tension, for motion involving 2 layers of water molecules, for $1/r^3$ and $1/r^6$ potentials. (b) As in panel a, but with 5 layers of molecules instead of 2.

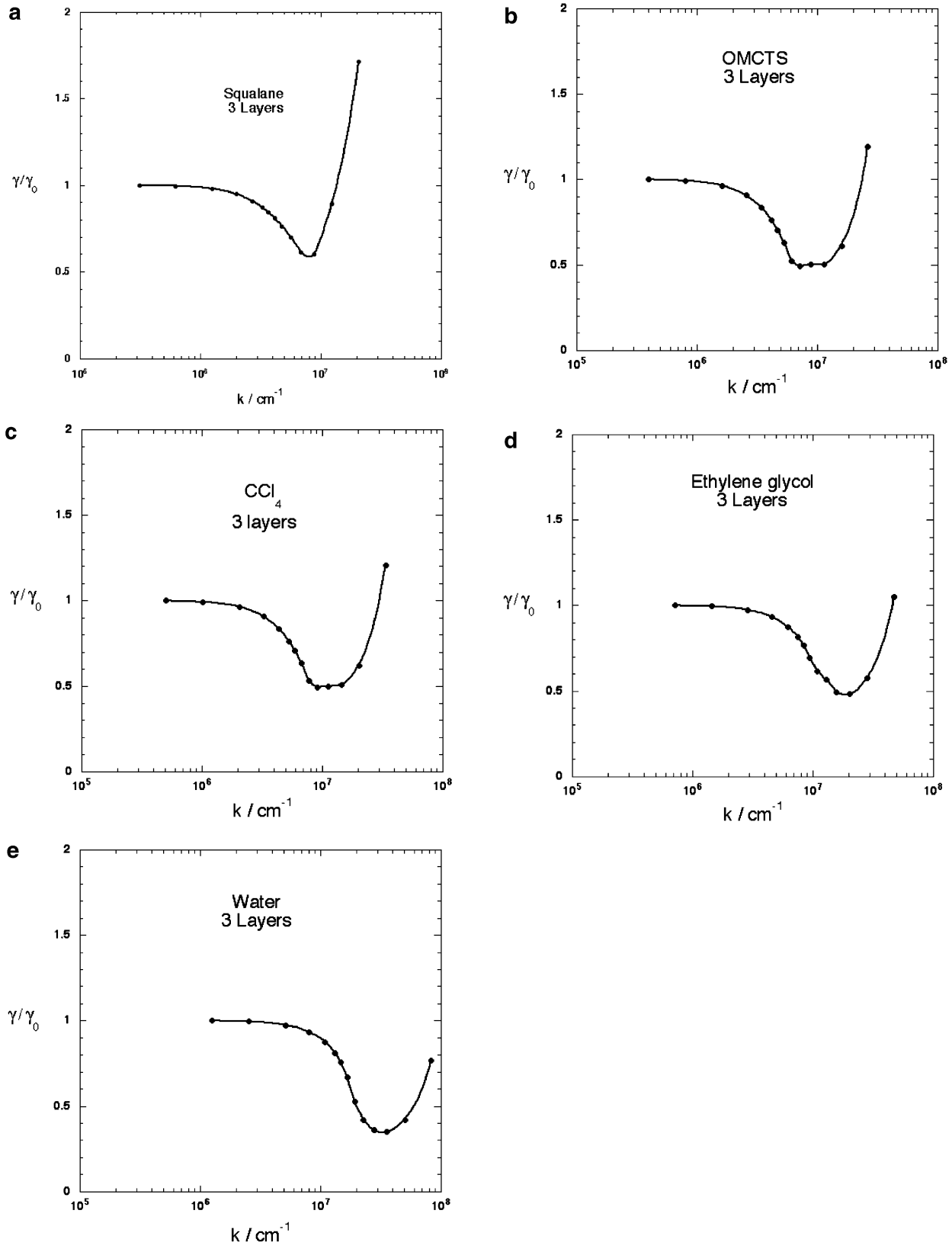

Figure 5. (a−e). Predicted dependence of the surface tension ratio γ/γ_0 on the wave vector for squalane, OMCTS, carbon tetrachloride, ethylene glycol, and water. The number of layers of surface molecules involved is 3.

Finally, the effective surface tension $\gamma(k)$ at a particular k-value was obtained from the equation

$$\langle h^2(k)\rangle/\langle h^2(0)\rangle = \gamma(0)/\gamma(k) \qquad (3)$$

where $\gamma(0)$ is the macroscopic value of surface tension and $\langle h^2(0)\rangle$ is the value of $\langle h^2(k)\rangle$ obtained with a very large dome radius (in practice, $n_r = 100$ was sufficient). In view of the simplicity of the model, the calculations were not expected to yield a priori values of $\gamma(0)$, but the predicted values of $\gamma(k)/\gamma(0)$ can still provide a useful test of the theory. Note that

no fitting is involved in the calculations and that the only parameters which enter are the molecular diameter σ and the macroscopic surface tension γ_0. Values used in the calculations are given in Table 1. All of the values of surface tension and the molecular diameters of water, OMCTS, and CCl_4 are from Mora et al.[7] The diameter of glycol was estimated from the values given by Hirschfelder, Curtiss, and Bird[12] for ethane and ethyl alcohol. The diameter of squalane was estimated by Koehler and McKendrick[13] from structural data in the NIST Webbook.[14] The *Chipmunk Basic* program that performs the calculations is available as Supporting Information.

Results and Discussion

Figure 4 shows calculated values of the surface tension ratio $\gamma(k)/\gamma(0)$ for water as a function of k for 2 and 5 layers of molecules (including the surface layer), for both $1/r^3$ and for $1/r^6$ potentials. Individual points on the curves correspond to the n_r values 100, 50, 25, 16, 12, 10, 9, 8, 7, 6, 5, 4, 3, and 2, where $n_r = 2$ corresponds to the smallest "dome" of Figure 1b, the one that appears in cross-section in Figure 1c. The four curves in Figure 4 are practically identical, which shows that the nature of the attractive potential is not very important and also that the calculation is not sensitive to the number of layers in which the anharmonic effects occur. This statement is still true when the number of layers is 10; higher values have not been tried. The rise in surface tension ratio at very high k-values is a consequence of the fact that large-amplitude motions at high k-values do not contribute to the observed rms displacement. Such motion is effectively truncated at the amplitude where the potential energy gradient changes sign, because larger amplitude motion leads to one or more surface molecules being either lost to vacuum or incorporated into the subsurface layer.

The present calculations do not consider thermal motions in the $x-y$ plane, parallel to the liquid surface, and do not consider bulk density fluctuations below the surface. Such motions would be expected to produce random variations in the effective molecular diameter and so tend to smear out the data along the k-axis, generally in the direction of lower k-value. The calculations also do not consider domes with more than one molecule per layer in the central column. Such domes would be expected to give data points at intermediate k-values.

Figure 5a−e shows surface tension ratios calculated for all of the liquids studied by Mora et al., using $1/r^3$ potentials for water and ethylene glycol and $1/r^6$ potentials for the others. In other respects these curves are similar to the ones in Figure 4. The curves that connect the calculated points are very similar to the experimental curves of Mora et al., the minimum values of the calculated surface tension ratio and the k-values at which the curves begin to rise sharply are similar to the experimental values, and the relative locations of the curves are well reproduced, with no adjustable parameters. Hence it seems reasonable to conclude that the enhanced surface roughness at high k-values is indeed due to the change from harmonic motion, with restoring force parallel to the surface, to anharmonic motion, with restoring force perpendicular to the surface, and it is interesting to observe that the only parameters upon which these curves depend are the molecular diameter and the macroscopic surface tension. The present work shows that the density functional theory calculations of Mora et al. are not invalidated by their assumption of a $1/r^6$ potential because the results are insensitive to the nature of the attractive potential. However, their emphasis on the importance of the long-range part of the attractive potential is probably incorrect.

In connection with the processes of evaporation and accommodation, the present calculations imply the existence of a symmetry between the two processes when they occur as a result of intense thermal excitation of small-scale capillary waves. In practice this symmetry is not observed, partly because the barriers to escape and accommodation are actually free-energy barriers and the entropy changes associated with evaporation and accommodation are very different. However, the main reason is that accommodation occurs over the whole spectrum of k-values, long-wavelength normal modes probably being most effective at bringing it about, because every oscillation of the surface results in the exchange of significant numbers of molecules between surface and bulk as a result of the creation or destruction of surface area. However, the idea that evaporation occurs as a result of small-scale capillary waves becoming thermally excited beyond the energy maximum in a highly anharmonic potential is interesting and probably worth pursuing.

Acknowledgment. The author gratefully acknowledges the support of the U.S. National Science Foundation (Grant No. 0209719).

Supporting Information Available: Chipmunk Basic program used to perform the calculations. This material is available free of charge via the Internet at http://pubs.acs.org.

References and Notes

(1) Buff, F. P.; Lovett, R. A.; Stillinger, R. H. *Phys. Rev. Lett*. **1965**, *15*, 621.
(2) Jungwirth, P.; Tobias, D. J. *J. Phys. Chem.* B **2002**, *106*, 6361.
(3) Fradin, C.; Braslau, D.; Luzet, D.; Smilgies, M.; Alba, N.; Boudet, N.; Mecke, K.; Daillant, J. *Nature* **2000**, *403*, 871.
(4) Phillips, L. F. *J. Phys. Chem. B* **2000**, *104*, 2534.
(5) Phillips, L. F. *J. Phys. Chem. B* **2001**, *105*, 11283.
(6) Mecke, K. *J. Phys. Condens. Matter* **2001**, *13*, 4615.
(7) Mora, S.; Daillant, J.; Mecke, K.; Luzet, D.; Braslau, A.; Alba, M.; Struth, B. *Phys. Rev. Lett.* **2003**, *90*, 216101/1.
(8) Robinson, G. W.; Zhu, S.-B.; Singh, S.; Evans, M. W. *Water in Biology, Chemistry, Physics*; World Scientific: Singapore, 1996.
(9) Silvestrelli, P. L.; Parrinello, M. *J. Chem. Phys.* **1999**, *111*, 3572.
(10) Gregory, J. K.; Clary, D. C.; Liu, K.; Brown, M. G.; Saykally, R. J. *Science* **1997**, *275*, 814.
(11) Gubskaya, A. V.; Kusalik, P. G. *J. Chem. Phys.* **2002**, *117*, 5290.
(12) Hirschfelder, J. O.; Curtiss, C. F.; Bird, R. B. *Molecular Theory of Gases and Liquids*; John Wiley & Sons Inc.: New York, 1954.
(13) McKendrick, K. G.; Koehler, S. Personal communication.
(14) http://webbook.nist.gov/cgi/cbook.cgi?ID=C111013&Units=SI.